Technical Report - Additional Experiment Results for Paper "Vehicle and Wheels Stability Defined Using Driving Envelope Protection Algorithm"

Denis Efremov, Martin Klaučo, and Tomáš Haniš [*]

1 Introduction

This document provides additional experiment results extending "Experiments" section of our submitted paper "Vehicle and Wheels Stability Defined Using Driving Envelope Protection Algorithm", submitted to IEEE TRANSACTIONS ON INTELLIGENT VEHICLES journal.

The mentioned paper aimed to utilize linear driving envelope [1] and model predictive control frameworks for vehicle stability. Provided simulation experiments show that the resulting control strategy could prevent wheel-locking, wheelspin, and wheel-skidding of all subjected wheels and overall of the vehicle. The experiments also show the robustness properties of the controller against a change of friction properties of the driving surface.

2 Experiment Setup

To simulate vehicle dynamics, we used IPG CarMaker software [2], which has compatibility with MATLAB/Simulink environment. The whole controller strategy from the paper is implemented in the Simulink environment. The optimal control problem is formulated in Matlab and is solved using the qpOASES [3] solver. We used "DemoCar" as the test vehicle, the most common vehicle in CarMaker. The whole project used for this paper with the implementation of control strategy in Matlab/Simulink environment is available on [git]. The test vehicle is operated by the basic programmed driver available in CarMaker software. We assume global brake and accelerator action with constant transfer between the pedal application and generated brake or drive torque on each wheel.

To test the hypothesis that the proposed control strategy could prevent vehicle dynamics' dangerous situations and provide functionality similar to ABS, TCS, and ESC systems at the same time, we offered four test scenarios in comparison to an uncontrolled car. Each test result and discussion are presented in the particular subsection.

All videos of provided ride test are published on our YouTube channel [youtube].

Used notation is presented in the Table 1.

[*]D. Efremov, M. Klaučo, and T. Haniš, are with Department of Control Engineering, Faculty of Electrical Engineering, Czech Technical University in Prague, 120 00 Nové Město, Czech Republic (e-mail: {denis.efremov, martin.klauco, tomas.hanis}@fel.cvut.cz

[†]M. Klaučo is with the Institute of Information Engineering, Automation, and Mathematics, Slovak University of Technology in Bratislava, Radlinskeho 9 82137 Bratislava, Slovakia (e-mail: martin.klauco@stuba.sk)

Variable	Symbol	Units
Vehicle velocity	v	$\mathrm{m\,s^{-1}}$
Sideslip angle	β	rad
Yaw rate	r	$\mathrm{rad\,s^{-1}}$
Brake pedal application	b	%
Throttle pedal application	t	%
Steering angle of front wheels	δ	rad
Angular velocity of wheel	ω	$\mathrm{rad\,s^{-1}}$
Load force	F_{z}	N
Traction force of wheel	$F_{\mathrm{x/y}}$	N
Sideslip angle of wheel	α	rad
Slip ratio of wheel	λ	–
Used subscriptions	**Subindex**	
Lateral or longitudinal direction	y or x	
Front or rear axle	f or r	
Left or right side	l or r	

Table 1: Used notation

3 Experiments

3.1 Sine with Dwell

We provided sine with dwell test to test electronic stability control (ESC) functionality and lateral vehicle stability. It induces oversteering motion of the vehicle. The experiment started once the car reached the predefined velocity (we used 80 km/h). The steering wheel did sine-like activation to the left and then to the right. At the maximum amplitude of the right position, it dwells for 0.5 s. Finally, the steering wheel returned to its original position (see reference signal in Fig. 1).

The baseline uncontrolled vehicle failed the test (Fig. 1) and went to a dangerous skid. On the other hand, the controlled vehicle successfully passed the test, as MPC predicatively simultaneously prevented boundary violations for sideslip angles of the front and rear wheels. The controller performed a fast front axle steering action in the direction of the skid. How fast the steering angle change is defined in the definition of the slew constrain in MPC. At the same time, the controller applied the throttle pedal to produce a longitudinal force on the front wheels. The throttle and brake pedal activations are rough due to small tracking weights for the front axle angular velocity and the prediction window size used for the MPC configuration. However, the prediction horizon is sufficient to prevent the dangerous vehicle's skid situation.

3.2 Acceleration on a Slippery Surface with Sudden μ Change

In the second scenario, we provided a test of wheelspin protection, which is a typical traction control system (TCS) functionality. We performed an acceleration test on a slippery surface with a sudden change to asphalt (Fig. 4). The experiment started with the vehicle on a low friction surface ($\mu = 0.4$) at a standstill. The uncontrolled vehicle over-spun the front axle due to the high engine torque. The baseline car outran the controlled one on the slippery surface. It is an effect of used tires: due to the shape of the slip curve presented in Fig. 2, the longitudinal traction force generated by the uncontrolled vehicle is a bit larger on the slippery part. However, when cars passed the slippery surface and came to the dry asphalt with nominal friction, the controlled vehicle outran the uncontrolled. It is the effect of unnecessary over-spun of driven wheels. Over-spun wheels must lose their angular velocity and "wait"

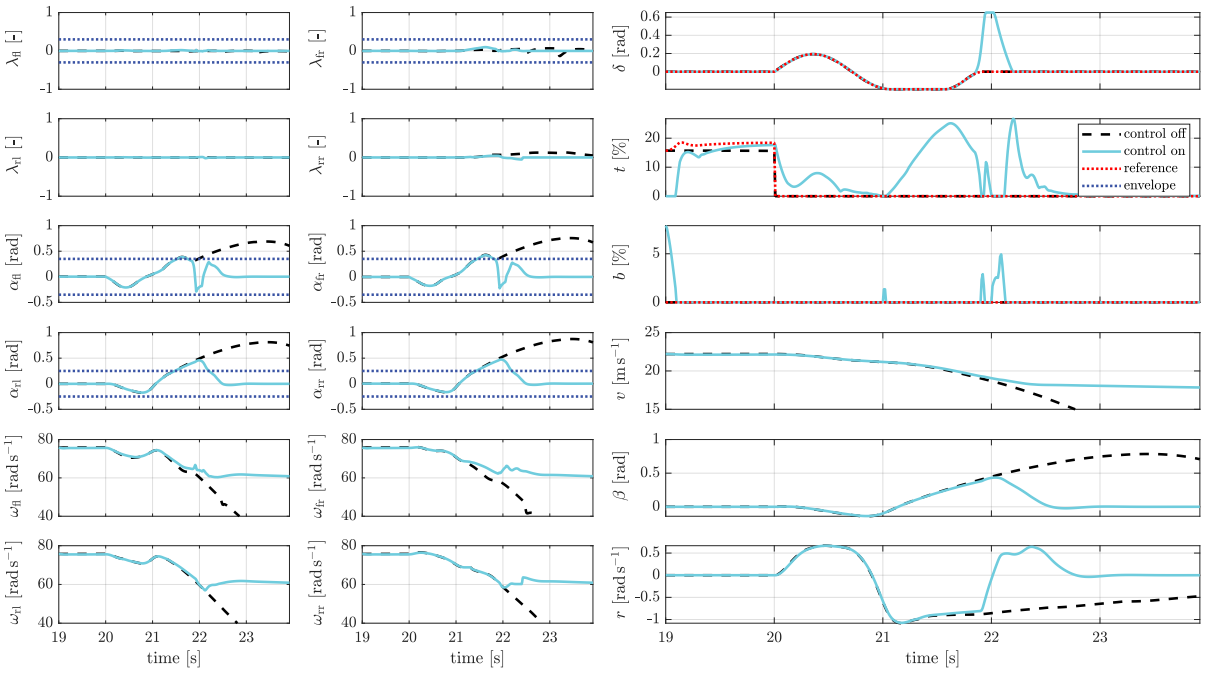

Figure 1: Sine with dwell at 80 km/h.

until the car's rigid body catches up wheel's velocity. The controller provides better slip ratio allocation to generate more traction force by the front wheels, which causes faster acceleration on the asphalt segment. Notice that the friction coefficient estimation did not provide during the experiment. Thus, the presented control structure contains robustness properties against the change of the friction parameters (or wheels' load forces.)

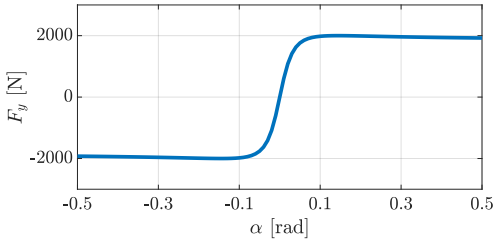

Figure 2: Longitudinal tire forces of test vehicle with load 2 kN.

Moreover, when the slip ratio of front wheels passes its peak value, the handling quality of front wheels in the lateral direction is significantly reduced because the lateral traction capabilities are exhausted. That could create dangerous situations once any lateral maneuver during acceleration is needed. Fig. 3 presents a car's heading deviation after a step-like change of the steering wheel position during acceleration on a slippery surface.

3.3 Full Stop during Cornering Maneuver

A corner braking test (Fig. 5) analyzes the controller's ability to help in fast braking situations while cornering. When the vehicle turns during braking, one side generates more longitudinal traction force than the other due to the car's rotation. Because of this, one front wheel (right in the experiment) was locking rapidly. Wheel-locking influenced the production of the lateral traction force. The driver could not stabilize the lateral vehicle dynamics using the steering wheel. All of these factors caused loss of vehicle maneuverability and sudden uncontrolled skidding behavior.

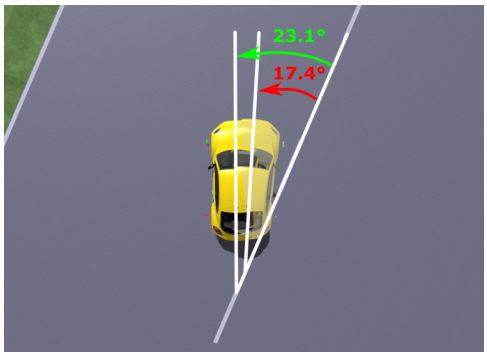

Figure 3: Lateral response of the vehicle with fully applied acceleration pedal. The ghost vehicle is uncontrolled. The yellow car is controlled by the proposed control structure.

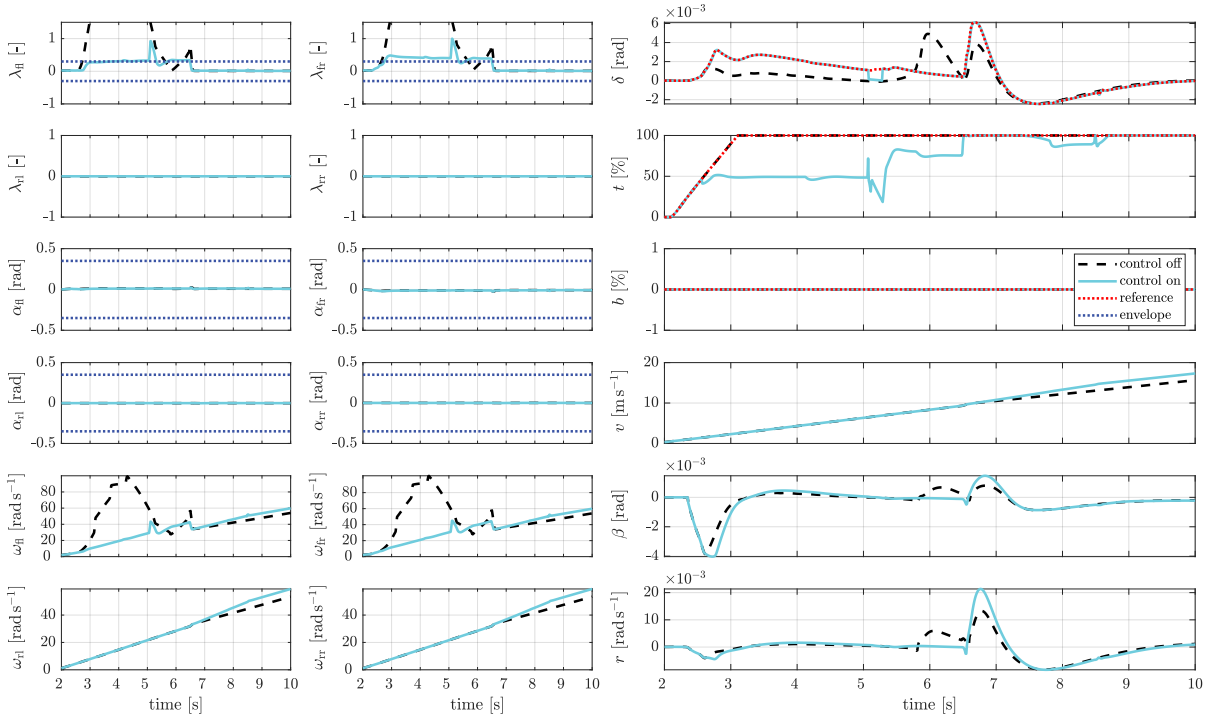

Figure 4: Acceleration on a slippery surface with $\mu = 0.4$ and sudden change to asphalt with $\mu = 1$ around 6.5 s.

On the other hand, the controlled vehicle did not lose traction because the front wheels stayed unlocked. It stopped without any loss of maneuverability. Notice that the used MPC did not protect the rear wheels. The right rear wheel was locked during the braking maneuver. Nevertheless, the proportion of load force on the front axle is significantly higher than on the rear axle. Thus, the rear slip ratio has a lower impact on the overall vehicle stability.

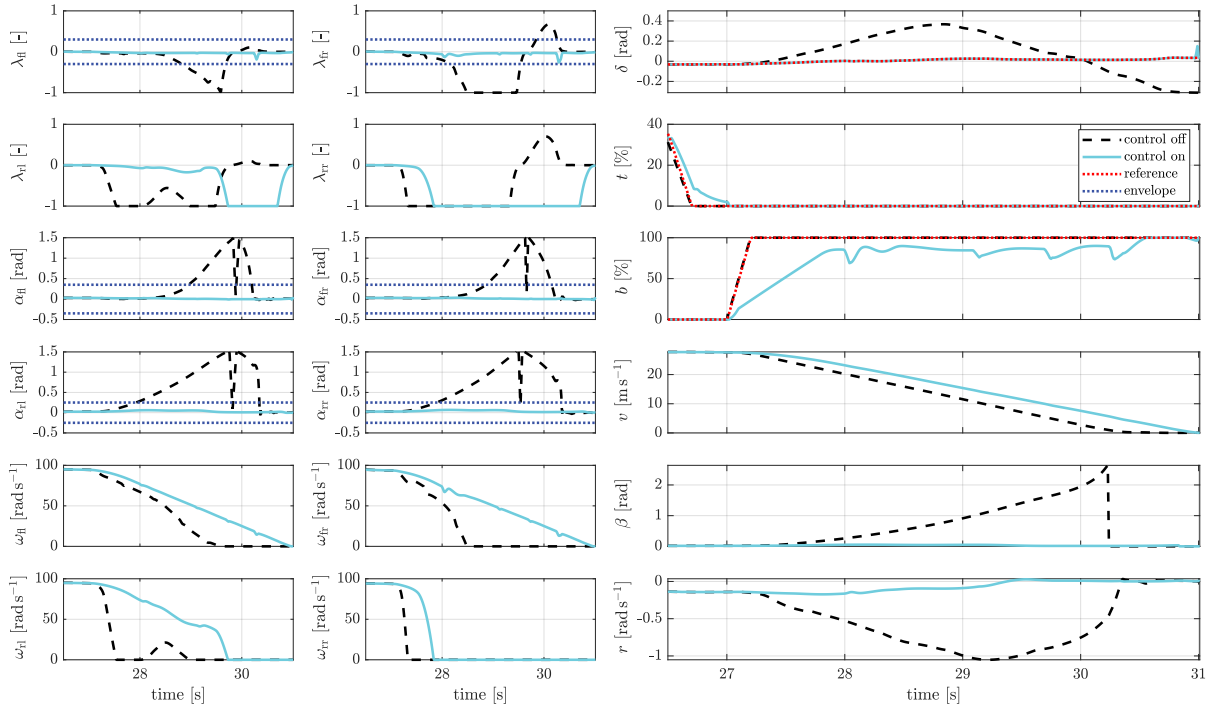

Figure 5: Braking on asphalt from 120 km/h during cornering maneuver.

3.4 Full Stop during Cornering Maneuver with μ-Split

To test the robustness of the used controller architecture, we enhanced the previously used corner braking test with a friction split pad (Fig. 6). The right side of the vehicle braked on a slippery surface with a friction coefficient equal to 0.4. The uncontrolled vehicle failed this test at the start of the braking maneuver due to locked right wheels. As a result, it suddenly went into an uncontrolled spin situation.

The controlled vehicle braked slower than in the previous test because it could not generate more traction force on the right side of the car. Nevertheless, the controller successfully prevented the locking of the front right wheel without knowing the traction capability of the drivable surface. Figure 7 presents normalized traction ellipses during this braking experiment. From this figure, we can admit that the reason for slower braking is the lower traction capacities of the right side of the car. The controlled vehicle did not violate the traction ellipse boundaries. However, it caused less braking force generated on the slippery surface. The uncontrolled car acted on the wheel mounting point with force, which the tire could not transfer to the place of contact with the surface. Thus, the traction ellipse boundary was violated, and the car suddenly went into an uncontrolled spin.

4 Acknowledgment

This work was supported in part by the Toyota Research on Automated Cars in Europe; in part by the Grant Agency of the Czech Technical University in Prague under Grant SGS22/166/OHK3/3T/13; in

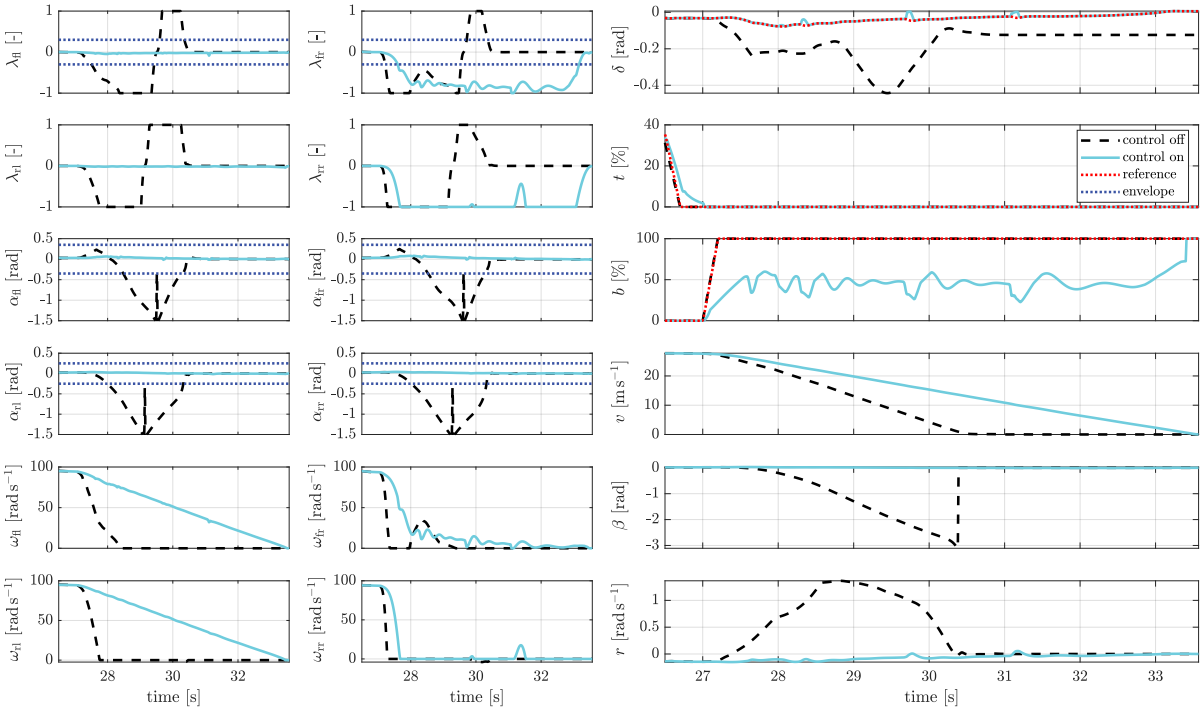

Figure 6: Braking on split surface from 120 km/h during cornering maneuver. The right side was on a slippery road with a friction coefficient equal to 0.4. The left side remained on asphalt with $\mu = 1$.

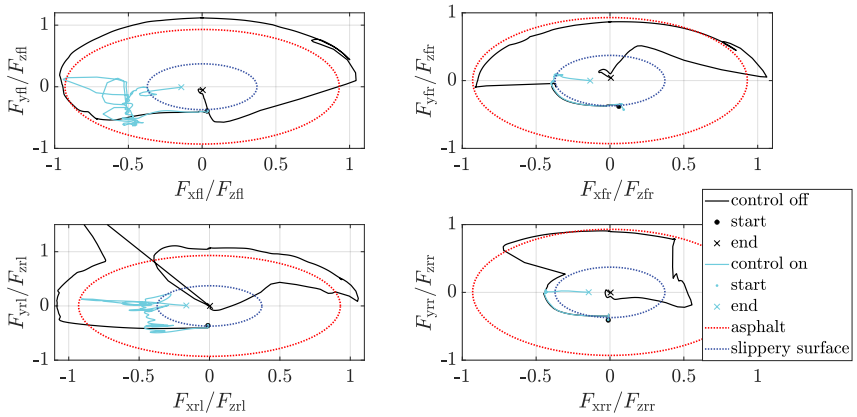

Figure 7: Normalized traction ellipses of wheels during split braking experiment.

part by the Slovak Research and Development Agency under Project Danube strategy 2019 DS-FR-19-0031 and APVV-20-0261; in part by the Ministry of Education, Youth and Sports of the Czech Republic under Project 8X20037.

References

[1] D. Efremov, M. Klaučo, T. Haniš, and M. Hromčík, "Driving envelope definition and envelope protection using model predictive control," in *Proc. of the American Control Conference*, Denver, CO, USA, 2020.

[2] IPG Automotive GmbH. (2022) Carmaker official website. [Online]. Available: https://ipg-automotive.com/en/products-solutions/software/carmaker/

[3] H. J. Ferreau, C. Kirches, A. Potschka, H. G. Bock, and M. Diehl, "qpoases: A parametric active-set algorithm for quadratic programming," *Mathematical Programming Computation*, vol. 6, no. 4, pp. 327–363, 2014.